Available online at www.sciencedirect.com
ScienceDirect
Journal of Sound and Vibration 317 (2008) 514–536
JOURNAL OF SOUND AND VIBRATION
www.elsevier.com/locate/jsvi

Hybrid balance control of a magnetorheological truck suspension

Georgios Tsampardoukas*, Charles W. Stammers, Emanuele Guglielmino[1]

Department of Mechanical Engineering, University of Bath, Flat 14, Cliffe Court, Rugby Road, Leamington SpaCV32 6DW, UK

Received 17 January 2007; received in revised form 14 March 2008; accepted 25 March 2008
Handling Editor: M.P. Cartmell
Available online 6 May 2008

Abstract

The paper concerns an investigation into the use of controlled magnetorheological dampers for a semi-active truck suspension. A control strategy targeted to reduce road damage without penalising driver comfort is presented. A half-truck model is employed and system performance investigated via numerical simulation. A balance control algorithm (variable structure-type algorithm) based on dynamic tyre force tracking has been devised. Algorithm robustness to parametric variations as well as to real-life implementation issues such as feedback signals noise are investigated as well.

The magnitude of total road damage reduction (over three axles) on a simulated random road varies with vehicle speed. The reduction was found to be 6% at 7.5 m s^{-1}, 19% at 17.5 m s^{-1} and 9% at 25 m s^{-1}.

1. Introduction

Heavy vehicle suspensions ought to be able to isolate the sprung mass from road-induced disturbances as well as improving handling and minimising road damage by reducing dynamic tyre force within the constraint of a set working space.

The sources of vehicle vibration are numerous, including road surface irregularities, aerodynamic forces and vibration arising from the rotating mechanical parts (tyres, engine, and power train).

Passive suspensions are typically employed in heavy vehicles. Woodrooffe [1], Cole and Cebon [2,3] and Cebon [4] examined the passive suspension design of a heavy vehicle to minimise road damage, as did Cole [5]. Queslati and Sankar [6] used covariance analysis and optimal control theory in order to determine the optimal suspension parameters. Optimisation with genetic algorithms was carried out by Vanduri and Law [7]. Cole et al. [8] and Ibrahim et al. [9] investigated thoroughly the dynamic interaction between the tractor and semi-trailer units.

*Corresponding author. Tel.: +44 1225 385962; fax: +44 1225 826928.
E-mail addresses: gdoukas1979@gmail.com (G. Tsampardoukas), C.W.Stammers@bath.ac.uk (C.W. Stammers), e.guglielmino@gmail.com (E. Guglielmino).
[1]At present with General Electric, Florence, Italy.

0022-460X/$ - see front matter © 2008 Elsevier Ltd. All rights reserved.
doi:10.1016/j.jsv.2008.03.040

Nomenclature

A_k^4 fourth power aggregate force
b_2 amount of the added pseudo-viscous damping, when control algorithm is ON
b_3 amount of critical damping when control algorithm is OFF
b_1 amount of dynamic tyre force cancellation
C_{bj} damper rate at the bound stroke
C_{rj} damper rate at the rebound stroke
C_{dj} critical damper rate, using damping ratio equal to unity
F_{cj} control force applied by SA damper to ith axle. $i = F$: tractor steering, $i = R$: tractor drive, $i = T$: Trailer
Fs_i suspension spring force to ith axle. $i = F$: tractor steering, $i = R$: tractor drive, ith $= T$: Trailer
F_{di} suspension damper force to ith axle. $i = F$: tractor steering, $i = R$: tractor drive, $i = T$: Trailer
I current input to the MRD
K_i suspension spring stiffness of ith axle, $i = F$: tractor steering, $i = R$: tractor drive, $i = T$: trailer
N_a number of axles on the vehicles
N_s number of measurement stations along the road
P_{jk}^4 force applied by the tyre jth at location k along the road
s road distance
S_g power spectral density
X_{wj} absolute heave displacement of the unsprung mass
X_j relative displacement between the unsprung mass and the sprung mass
X_5 relative displacement between the tractor and the trailer sprung mass

Greek letters

Θ_C absolute pitch displacement of the tractor sprung mass
Θ_T absolute pitch displacement of the trailer sprung mass
Ω spatial frequency

Amongst controlled suspension systems a semi-active suspension, usually composed of a controlled damper in parallel with a passive spring, offers a relatively low-cost and reliable solution. A number of control schemes have been proposed for semi-active suspensions over the years.

The authors initially explored the use of controlled friction dampers (FD) in automotive applications [10–12] and have subsequently focussed their research effort on magnetorheological dampers (MRD). Guglielmino et al. [13,14] give results for vehicles and, most recently, for trucks.

Details of MRD performance and MR fluids properties are given in Dyke et al. [15], Spencer et al. [16], Choi et al. [17] and Agrawal et al. [18]. In the automotive field they are amongst the most promising devices for use in semi-active suspensions. The literature in the field is extensive; see for instance Kelso and Gordaninejad [19], Lee and Choi [20], and Lau and Liao [21].

Controlled suspensions were first investigated by Karnopp et al. [22] who originally devised the skyhook damping logic. Similar work was performed by Alanoly and Sankar [23] and Rakheja and Sankar [24] in terms of active and semi-active isolators. The most attractive feature of that work was that the control strategies were based only upon the measurement of the relative displacement and velocity. A review can be found in Crolla [25]. Recently Liu et al. [26] studied four different semi-active control strategies mainly based on the skyhook and balance control algorithms.

The reduction of dynamic tyre forces is a challenging field. Cole et al. [8] did extensive work, both theoretical and experimental. Extended groundhook control logic was also investigated by Valasek et al. [27] in order to reduce the dynamic tyre forces.

Related work was performed by Hendrick and Yi [28] and Yi and Song [29] who developed a novel control called road detection algorithm (RDA). The aim of this algorithm was to combine the advantages of the skyhook damping and the tyre deflection feedback. A comparative study was performed by Margolis and Nobles [30] in order to control the heave and roll motions of large off-road vehicles.

The algorithms presented here are aimed at the reduction of tyre load oscillations, which improves handling and reduces road damage caused by vehicle wheels. This latter application is particularly important in the case of heavy freight vehicles.

The aim of this paper is to present a hybrid balance algorithm to reduce road damage and to investigate the performance of a heavy articulated vehicle equipped with MR dampers compared to one with passive viscous dampers.

The algorithm used is of variable structure-type, a class of robust algorithms. Robustness to parametric uncertainties as well as to superimposed noise on the feedback signals has been assessed.

2. Half-truck model

Extensive simulation work has been carried out on a half-truck model. The analytical model of the heavy articulated vehicle is presented in Fig. 1. The system is modelled as a three-axle vehicle, the steering axle, the tractor drive axle and the trailer axle, assuming two MR dampers, one fitted on tractor drive axle and the other on the trailer axle. The steering axle is equipped with a passive viscous damper.

Linear springs are employed at each axle and the articulation connection (5th wheel) is also modelled as a high stiffness spring and damper. Both vehicle units are assumed to be rigid bodies [31].

The objective is to investigate the vehicle performance for various road profiles in terms of ride and road damage using two semi-active dampers controlled by hybrid logic. The heavy articulated vehicle travels in a straight line with constant speed. Hence, lateral and yaw motions are neglected at this stage, reducing the model complexity. Roll motion is also neglected as the effect is small, especially when the vehicle travels over smooth highways.

The equations of motion describing the coupled motion of both vehicle units (sprung masses) can be written as

$$M_C\ddot{X}_C - K_F X_1 - C_F\dot{X}_1 - K_R X_2 - C_R\dot{X}_2 + K_5 X_5 + C_5\dot{X}_5 = 0 \tag{1}$$

$$M_T\ddot{X}_T - K_T X_3 - C_T\dot{X}_3 - K_5 X_5 + C_5\dot{X}_5 = 0 \tag{2}$$

$$I_C\ddot{\Theta}_C - L_2K_R X_1 - L_2C_R\dot{X}_1 + L_1K_F X_1 + L_1C_F\dot{X}_1 + L_5K_5 X_5 + L_5C_5\dot{X}_5 = 0 \tag{3}$$

$$I_T\ddot{\Theta}_T - L_6K_T X_3 - L_6C_T\dot{X}_3 + L_5K_5 X_5 + L_5C_5\dot{X}_5 = 0 \tag{4}$$

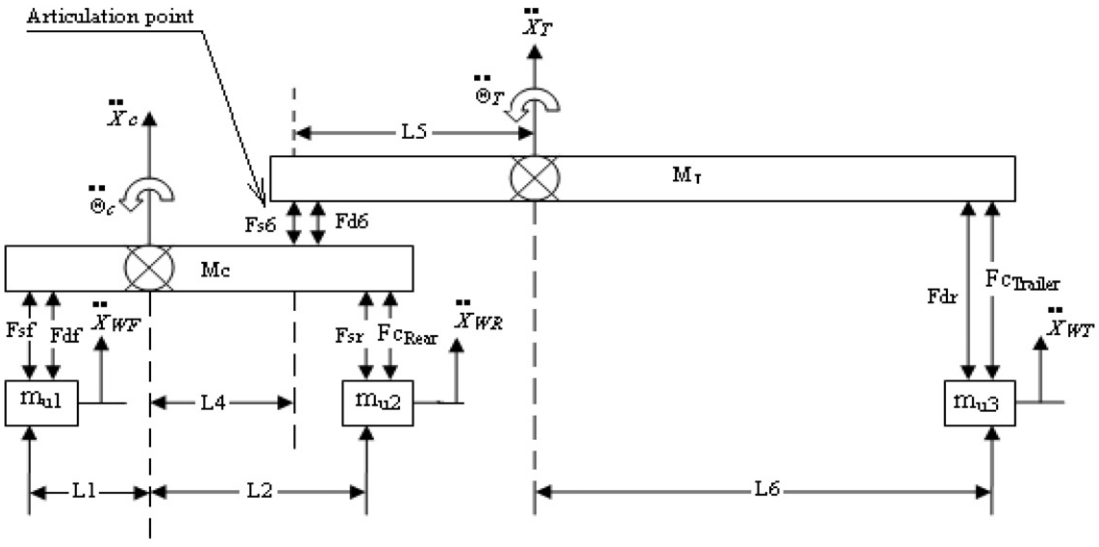

Fig. 1. Schematic diagram of the half-truck vehicle model.

The relative displacements and velocities are given by

$$X_1 = X_{wf} - X_C + L_1\Theta_C \tag{5}$$

$$\dot{X}_1 = \dot{X}_{wf} - \dot{X}_C + L_1\dot{\Theta}_C \tag{6}$$

$$X_2 = X_{wr} - X_C - L_2\Theta_C \tag{7}$$

$$\dot{X}_2 = \dot{X}_{wr} - \dot{X}_C - L_2\dot{\Theta}_C \tag{8}$$

$$X_3 = X_{wt} - X_T + L_6\Theta_T \tag{9}$$

$$\dot{X}_3 = \dot{X}_{wt} - \dot{X}_T + L_6\dot{\Theta}_T \tag{10}$$

$$X_5 = X_C + L_4\Theta_C - X_T + L_5\Theta_T \tag{11}$$

$$\dot{X}_5 = \dot{X}_C + L_4\dot{\Theta}_C - \dot{X}_T + L_5\dot{\Theta}_T \tag{12}$$

Analogous equations can be written for the unsprung masses. The system response is obtained by directly integrating the equations of motion. Simulations were carried out in MATLAB® and Simulink® using a fourth-order Runge–Kutta integration method with variable time step. The numerical parameters employed in simulation are listed in Appendix A.

2.1. Road damage assessment

Weather conditions as well as vehicle motion are two key causes of road pavement damage. However, dynamic forces transmitted to the road surface are a major cause of road failure. A thorough analysis of the damage due to dynamic tyre forces and other co-factors is presented by Cebon et al. [3,4]. An instrumented vehicle was employed to measure the dynamic tyre forces at both low and high excitation frequencies. The study concluded that the wheel dynamic load increases with both vehicle speed and road roughness.

It is of paramount importance to establish a quantitative criterion to assess road damage. The most widely employed is the fourth power law. This is a result of the experimental work undertaken by the American Association of State Highway and Transportation Officials (AASHO) [31]. This law shows that the pavement serviceability decreases every time a heavy vehicle axle passes on the road. This reduction is assumed to be related to the fourth power of its static load [4]. Another criterion known as the "aggregate fourth power force" is described by Cole et al. [8] and Potter et al. [32] give a simplified approach to road damage. It is expressed by

$$A_k^n = \sum_{i=1}^{N_a} P_{jk}^n \tag{13}$$

where k is the location along the road and N_a is the number of axles. The exponent n is dependent on the type of pavement and ranges from $n = 4$ (suitable for fatigue damage) to $n = 1$ (permanent deformation caused by static load). In this work in order to describe the fatigue damage, the aggregate fourth power law with $n = 4$ is used, normalised with respect to the static force.

2.2. MR damper model

A variety of MRD models have been developed to capture damper nonlinear behaviour including the Bingham model, several Bouc–Wen-based models [15] and more recently neural network techniques [33]. The MRD model presented here is based on a work by Lau and Liao [21] who designed and modelled a prototype damper for a train suspension. Such a damper develops forces of the same order of magnitude as those required in a truck application and in this respect it could be potentially suitable for heavy vehicle applications as well.

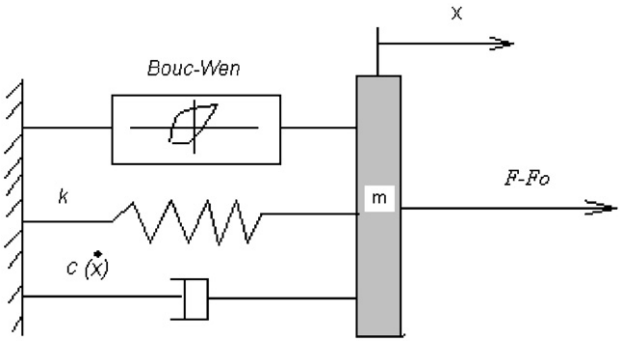

Fig. 2. Schematic model of MRD.

The schematic diagram of the damper model is shown in Fig. 2. It is a Bouc–Wen model coupled with a nonlinear viscous damper having exponential characteristics and a linear spring term. Eqs. (14)–(16) describe the Bouc–Wen model which is used in the simulation process

$$\dot{z} = -\gamma|\dot{X}|\,|z|^{n-1}z - \beta\dot{X}|z|^{n} + A\dot{X} \tag{14}$$

$$C = a_1\,\exp\{-(a_2\dot{X})^{p}\} \tag{15}$$

$$F = az + kX + C\dot{X} + m\ddot{X} + F_0 \tag{16}$$

where m is a mass to emulate the MR fluid inertia effect, k the accumulator stiffness and F_0 is the damper seal friction force or accumulator offset force. X is the excitation displacement of the MR damper.

The variable z is an evolutionary variable while the parameters β, γ, A and n define the shape of the hysteresis loop Eq. (15) models the post-yield plastic damping coefficient which depends on the relative velocity and from the parameters a_1, a_2 and p (parameters which determine the shape of the hysteresis loop). This equation is used to describe the MR fluid shear thinning effect, which results in the roll-off of the resisting force of the damper in the low-velocity region. The total exerted force is described by Eq. (16), which takes into account the evolutionary variable z and the post-yield plastic model, expressed by Eq. (15).

Tables 1 and 2 list the numerical value of the equation coefficients. Table 1 gives parameter values for terms independent of current and Table 2 those for current-dependent terms.

The simulated characteristics are depicted in Figs. 3 and 4 for two different excitation inputs.

The mathematical model of the passive viscous damper used in the simulation is described by

$$F_{d,j} = \begin{cases} C_{b,j}\dot{X}_j & \text{if } \dot{X}_j > 0 \\ C_{r,j}\dot{X}_j & \text{if } \dot{X}_j < 0 \end{cases} \tag{17}$$

Different damping coefficients have been selected for the bound and rebound strokes; the equivalent damping ratios are 0.15 and 0.35 for closure and rebound, respectively.

2.3. Road profile

Appropriate road profile models are required to assess truck performance under realistic operating conditions. Two types of road were considered: a smooth highway and a gravel highway. The spectral densities of both road profiles are expressed by

$$Sg(\Omega) = C_{sp}\Omega^{-N} \tag{18}$$

where C_{sp} and N determine the road quality (e.g. $C_{sp} = 4.8 \times 10^{-7}$ and $N = 2.1$ for a smooth highway or $C_{sp} = 4.4 \times 10^{-6}$ and $N = 2.1$ for a road with gravel). In this study, the numerical values for smooth highway and gravel road are those proposed by Wong [34]. While heavy good vehicles are usually designed to operate

Table 1
Constant parameters for MR damper

Parameter	Value (m^{-1})	Parameter	Value
γ	32000	m	100 kg
β	22	k	2.5 kN m^{-1}
A	220	p	0.54

Table 2
Current-dependent parameters of MR damper

Current (A)	a (kN)	a_1 (kN s m^{-1})	a_2 (s m^{-1})	n	f_o (kN)
0.5	15	32	6	2.7	0.4
1	27	65	8	2.7755	0.5
1.5	40	85	8	2.7755	0.5

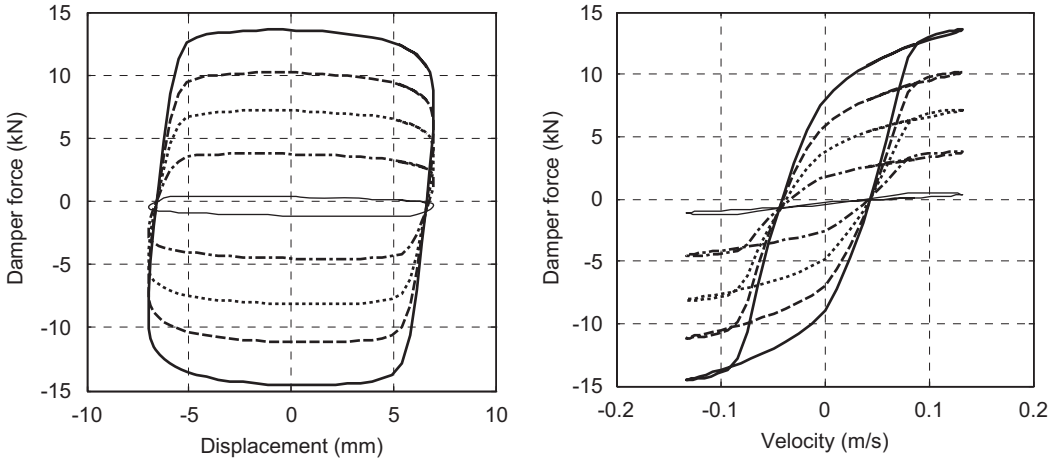

Fig. 3. Sinusoidal excitation displacement with amplitude 0.007 m and 3 Hz frequency: (——) 2 A, (– – –) 1.5 A, (- - - -) 1 A, (– – – -) 0.5 A, (——) 0 A.

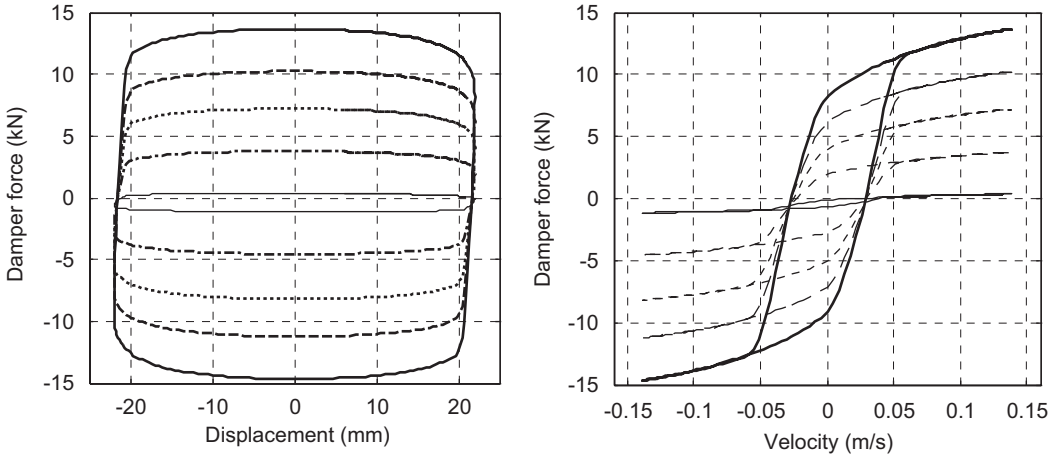

Fig. 4. Sinusoidal excitation displacement with amplitude 0.022 m and 1 Hz frequency: (——) 2 A, (– – –) 1.5 A, (- - - -) 1 A, (– – – -) 0.5 A, (——) 0 A.

on smooth rather than on poor roads, vehicle operation on highway with gravel is a scenario to examine the performance of the semi-active suspension on damaged roads or in off-road operation.

2.4. Semi-active control algorithm (balance control)

The essence of the proposed control algorithm is to cancel the tyre force fluctuations on each axle by ensuring that the wheel follows the road profile closely. The dynamic tyre forces are balanced by applying a controlled damping force in the opposite direction. This is only possible when the required control force and the relative velocity have opposite signs and hence energy dissipation takes place. A hybrid version of balance control is presented by Eq. (19) aimed at cancelling the drive tractor and trailer axle tyre forces

$$F_{C,j} = \begin{cases} -b_1(K_i X_j + m_{uj}\ddot{X}_j) + b_2 C_{d,j},\ \dot{X}_j & \text{if } F_{C,j}\dot{X}_j < 0 \\ b_3 C_{d,j}\dot{X}_j & \text{if } F_{C,j}\dot{X}_j > 0 \end{cases} \tag{19}$$

A pseudo-viscous damping term is added to the control force to reduce transients particularly when inputs are near the wheel-hop frequency. Numerical simulations (not shown here) have indicated that the optimal values of b_2 and b_3 (to minimise road damage) should be 20% of the critical passive damping when the vehicle travels on smooth or gravel roads. Smaller or higher values of b_2 and b_3 result in larger dynamic tyre forces and higher vibration levels. However, the optimum value of those parameters alters when the vehicle wheels come into contact with bumps or potholes. In case of a pothole, the optimum force cancellation is reduced to 50–60% and the pseudo-viscous damping ratio increases from 0.2 to 0.5 of its critical value ($\zeta = 1$).

3. Numerical results

3.1. Time response

To check the performance of the MR damper, the time response to a 5-mm amplitude 2-Hz sinusoidal road input surface was considered (Fig. 5). Hybrid control logic reduces the dynamic tyre forces of the tractor drive and trailer axles significantly at the expense of introducing some higher frequency components. The same trend is also observed for the trailer chassis acceleration. In contrast, the controlled suspension increases chassis acceleration of the tractor unit, as is discussed below, for a realistic road profile.

3.2. Vehicle response (random road input)

In this section, and in the following ones, the response of the semi-active controlled MRD system is benchmarked against the passive system. The passive MR damper (i.e., when zero current is applied to the MR damper—for instance in case of failure of the control system) is also considered.

In Fig. 6 the rms pitch and heave accelerations for tractor and trailer over a range of vehicle velocities are plotted. Also included is the case of a passive (failed) MR damper ($I = 0$ A). A smooth highway road profile was chosen. The semi-active MR damper is directed so as to cancel 100% of the tyre force fluctuations with the time constant T_c of the first-order lag (accounting for electromagnetic dynamic response) set at 11 ms (time to reach 64% of step demand). This value was drawn from Ref. [39]. The issue of MR damper time constant is discussed in Section 3.2.2.

It should be noted that the semi-active suspension actually increases tractor chassis accelerations since the controllable damper is installed on the drive tractor axle only. It has been verified that the tractor performance would improve if a third MR damper was fitted on the steer axle as well. However, truck driver seats are often equipped with a seat damper (not modelled in this work) which in practice reduces the vibration level experienced by the driver.

Because of the low damping produced by the failed damper, there is a resonant condition at a vehicle speed of 17.5 m s^{-1} due to wheel-hop.

The percentage reduction in trailer pitch and heave acceleration achieved by the semi-active case relative to the passive case is given in Table 3 for vehicle speeds of 7.5 m s^{-1} (27 km h^{-1} or 16.77 mph), 17.5 m s^{-1}

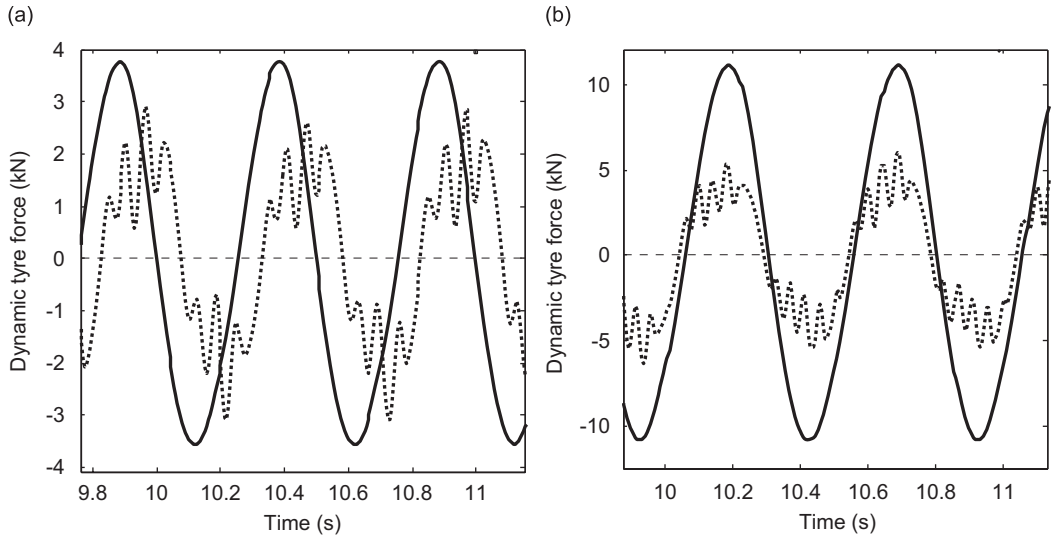

Fig. 5. Dynamic tyre forces on tractor drive and trailer axle: (a) tractor drive axle. (b) trailer axle: (-----) semi-active, (——) passive.

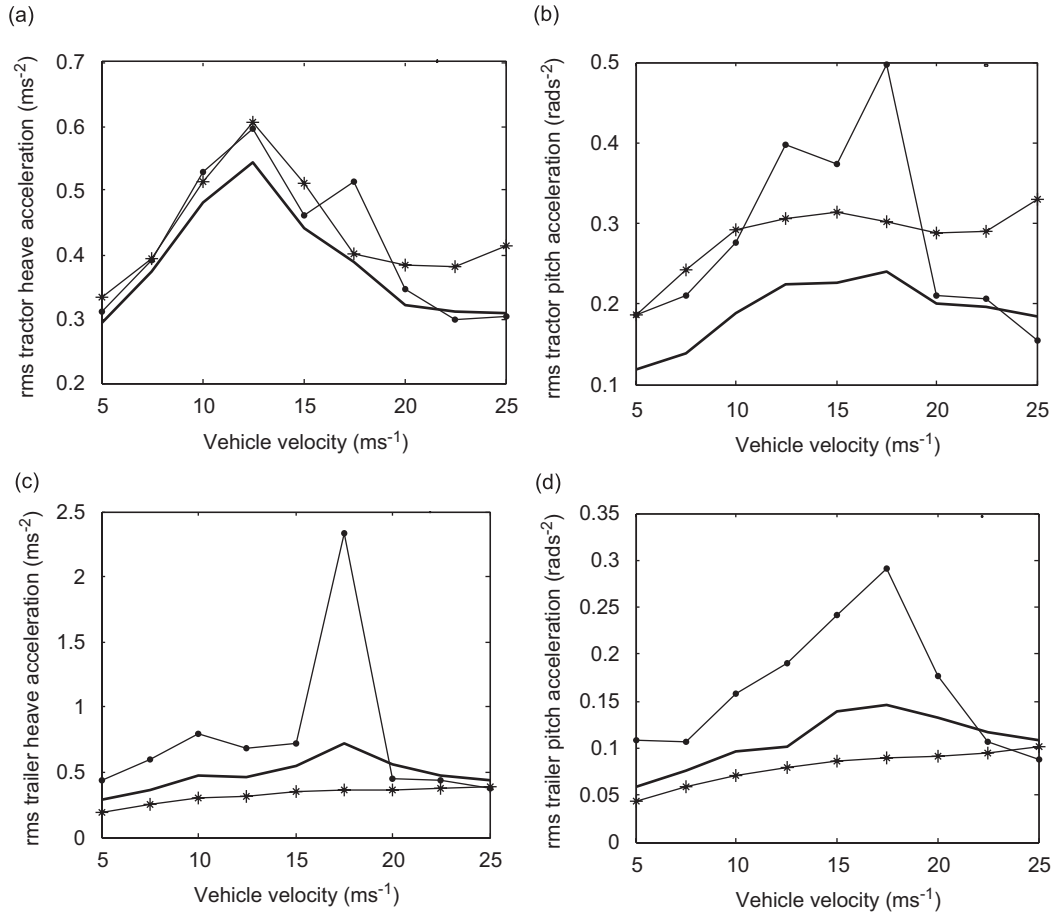

Fig. 6. The rms heave and pitch acceleration: (a) tractor chassis, (b) tractor chassis, (c) trailer chassis, (d) trailer chassis: (——) conventional passive viscous damper, (—●—) passive MR damper (current = 0 A), and (—✳—) semi-active MR damper.

Table 3
Percentage reduction in heave and pitch acceleration

Vehicle velocity ($m\,s^{-1}$)	rms trailer heave acceleration ($m\,s^{-2}$) (%)	rms trailer pitch acceleration ($rad\,s^{-2}$) (%)
7.5	58	20
17.5	70	40
25	−10	9

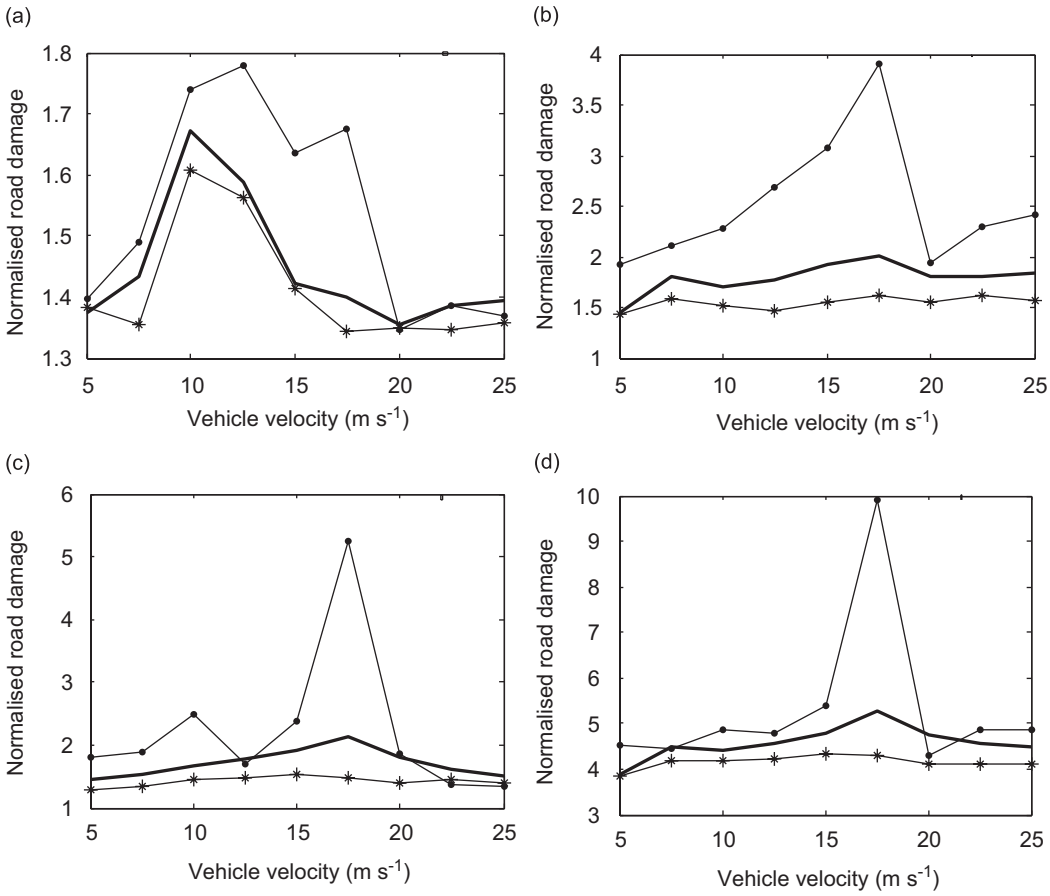

Fig. 7. Maximum normalised road damage: (a) steer axle, (b) drive axle, (c) trailer axle, (d) total vehicle: (——) conventional passive viscous damper, (—✱—) passive MR damper (current = 0 A), and (—✱—) semi-active MR damper.

(63 km h^{-1} or 39.14 mph) and 25 m s^{-1} (90 km h^{-1} or 56 mph). The second speed was chosen because of the wheel-hop resonance evident in this case. The semi-active MR damper reduces the trailer unit acceleration significantly due to the improved isolation achieved by the MR dampers fitted on the drive tractor and trailer axles.

Plots of maximum road damage are shown in Fig. 7 as a function of speed, and summarised in Table 4 for vehicle speeds of 7.5, 17.5 and 25 m s^{-1}. The damage caused by the dynamic tyre forces is significantly reduced when balance control is set to fully cancel the dynamic tyre forces while the parameters b_2 and b_3 (see Eq. (16)) are set to 0.2 of the critical damping force. It is important to note that a passive (failed) MR damper (i.e., $I = 0$ A) produces significant road damage at 17.5 m s^{-1} as a result of a wheel-hop resonance which produces the relatively high chassis accelerations discussed above.

The range of the damper force demanded by a controlled truck suspension must be known in order to select an appropriately sized MR damper. Fig. 8 compares the required semi-active damper force with the passive

Table 4
Percentage reduction of maximum road damage: tractor drive axle, trailer axle and total

Vehicle velocity ($m\,s^{-1}$)	Semi-active relative to conventional passive damper		
	Tractor (%)	Trailer (%)	Total vehicle (%)
7.5	12	11	6
17.5	19	29	19
25	15	7	9

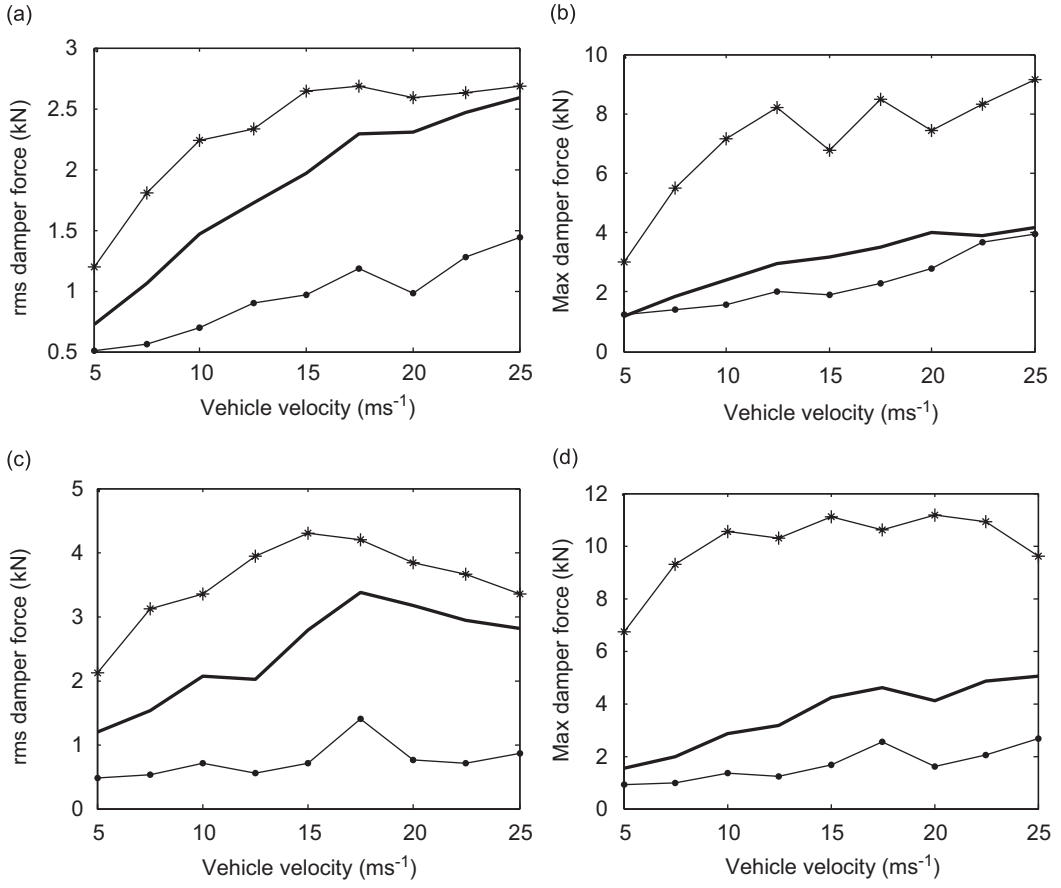

Fig. 8. Required semi-active damper force vs. passive damper: (a) drive axle (rms values), (b) drive axle (MAX values), (c) trailer axle (rms values), (d) trailer axle (MAX values): (——) conventional passive viscous damper, (—●—) passive MR damper (current = 0 A), and (—✶—) semi-active MR damper.

damper force for this application. The rms and MAX values of semi-active damper are almost double those in a passive suspension system with a conventional viscous damper. It should be also noted that the maximum available passive MR damper force is much lower than the conventional viscous damper and this is the main reason why the passive MRD degrades the vehicle response.

3.2.1. The effect of partial cancellation

The amount of dynamic tyre force cancellation is a critical parameter, which affects the system response as Fig. 9 shows. 100% cancellation is the best option at low and medium vehicle speeds because both rms and MAX dynamic tyre forces at each axle are significantly reduced relative to passive system, resulting in lower road damage with respect to the damage criterion used. On the other hand, it is beneficial to reduce the

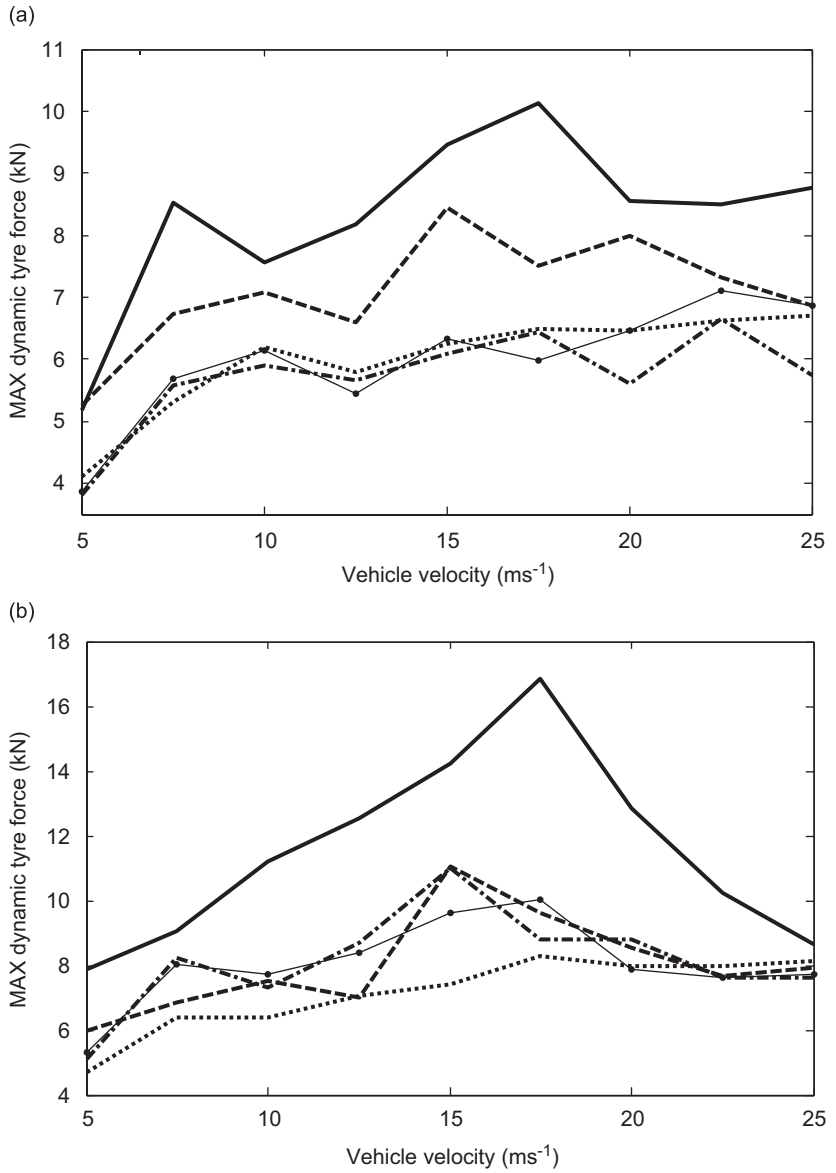

Fig. 9. MAX dynamic tyre forces due to partial cancellation: (a) tractor drive axle, (b) trailer axle: (——) passive viscous damper, (– – –) semi-active 25% cancellation, (- - - -) semi-active 50% cancellation, (– – –-) semi-active 75% cancellation and (——●——) semi-active 100% cancellation.

amount of cancellation for the damper fitted on the tractor drive axle in order to improve tractor unit comfort, particularly at high vehicle velocities, but such a reduction adversely affects road damage at high velocities.

Consequently, the optimum choice for the amount of spring force cancellation depends on the control objective. Similar work published by the authors [40] has shown that optimum ride is always obtained using skyhook control instead of the hybrid balance control. The reduction of the road damage is the main objective of this paper; hence the hybrid balance control algorithm is the best choice because of the significant reduction of the MAX and rms dynamic tyre forces.

A design solution which achieves a compromise between these two requirements entails the use of a suspended driver cab and seat to help reduce the vibration levels transmitted to the human body. In that case, 75% cancellation is the best solution in terms of lower MAX dynamic tyre forces for the semi-active device located at the tractor drive axle, while 50% cancellation is the best solution overall for the same device at the

trailer axle. The variation between the amount of cancellation between the units is mainly affected by the vehicle motion and the model (half truck) used. Consequently, a full truck model should be developed for future simulations in order to evaluate the performance of the hybrid control logic not only for ride but also in handling manoeuvres including roll motion.

3.2.2. Vehicle response on gravel road

Even a smooth road surface may have sections where the surface is rough due to lack of maintenance or due to resurfacing work. Consequently, vehicle operation on highway with gravel is a scenario to assess the performance of the semi-active suspension either "off road" or on a poorly maintained road.

Simulation results show that the heave and pitch accelerations of the tractor and trailer units are reduced by control. Fig. 10 presents the dynamic tyre forces of the vehicle in the three cases considered (passive, failed MR and working MR damper). The semi-active suspension performs better than the passive system over the velocity range investigated; however, the control logic becomes ineffective when the vehicle velocity is higher than $25\,\mathrm{m\,s^{-1}}$. This is probably because the frequency of road input is too high with respect to the MR damper-based control system bandwidth.

The vehicle performance is similar to that on smooth road in terms of normalised road damage. The results presented so far can be summarised as follows:

1. Semi-active hybrid balance control is beneficial to heavy vehicle performance: road damage as well as chassis acceleration are significantly reduced.
2. The semi-active MR damper significantly reduces axle loads at all speeds on both rough and smooth roads.
3. Employing balance control algorithm on the drive tractor and trailer controlled dampers results is a substantial reduction of trailer chassis acceleration. The tractor chassis acceleration slightly increases because a passive viscous damper is used on the steer tractor axle.
4. The optimal partial cancellation of the dynamic tyre forces is a function of the vehicle speed. The optimal solution in terms of lower road damage in the moderate vehicle speed range (from 12.5 to $20\,\mathrm{m\,s^{-1}}$) is 100% cancellation, while 75% cancellation is the best solution in the low (from 5 to $10\,\mathrm{m\,s^{-1}}$) and high vehicle speed ranges (from 20 to $25\,\mathrm{m\,s^{-1}}$).
5. The passive MR damper (electrical current equal to 0 A) is not able to produce high forces resulting in excessive load on axles. However a MR damper operates in this mode only if the control system power supply fails. The system performs poorly but this is a provisional fail-safe condition. The on-board electronics would spot the failure immediately and send a warning to the driver.

3.2.3. Vehicle response to pothole and bump

It is important to obtain the vehicle response to bump and pothole inputs. The bump and pothole are modelled [35] as follows:

$$r(s) = \begin{cases} -\dfrac{a}{2}\left[1 - \cos\dfrac{2\pi s}{b}\right], & 0 < s < b \\ 0, & s < 0,\ s > b \end{cases} \tag{20}$$

The parameters a and b determine the depth and the width of the pothole ($a = 0.03\,\mathrm{m}$ and $b = 1\,\mathrm{m}$), while the negative value of a corresponds to a bump ($a = -0.03\,\mathrm{m}$ and $b = 1\,\mathrm{m}$).

Figs. 11 and 12 show that the semi-active control scheme reduces the peak values of the dynamic tyre forces on the trailer axle. A similar result holds for the tractor drive axle (graphs not shown). The controlled suspension reduces the number of oscillations with respect to the passive suspension. Similar trends can be observed for vehicle velocity ranging from 5 to $25\,\mathrm{m\,s^{-1}}$ (results not shown in the paper). The amount of cancellation used in this study is 100% with additional pseudo-viscous damping ratio of 0.5.

An improvement is observed as well on the trailer body heave acceleration (Fig. 13). Pitch acceleration is also reduced (graphs not shown here); the free oscillations are significantly reduced with the semi-active control as this result in additional damping. The pitch responses to the bump are similar to that in heave and hence the graphs are omitted.

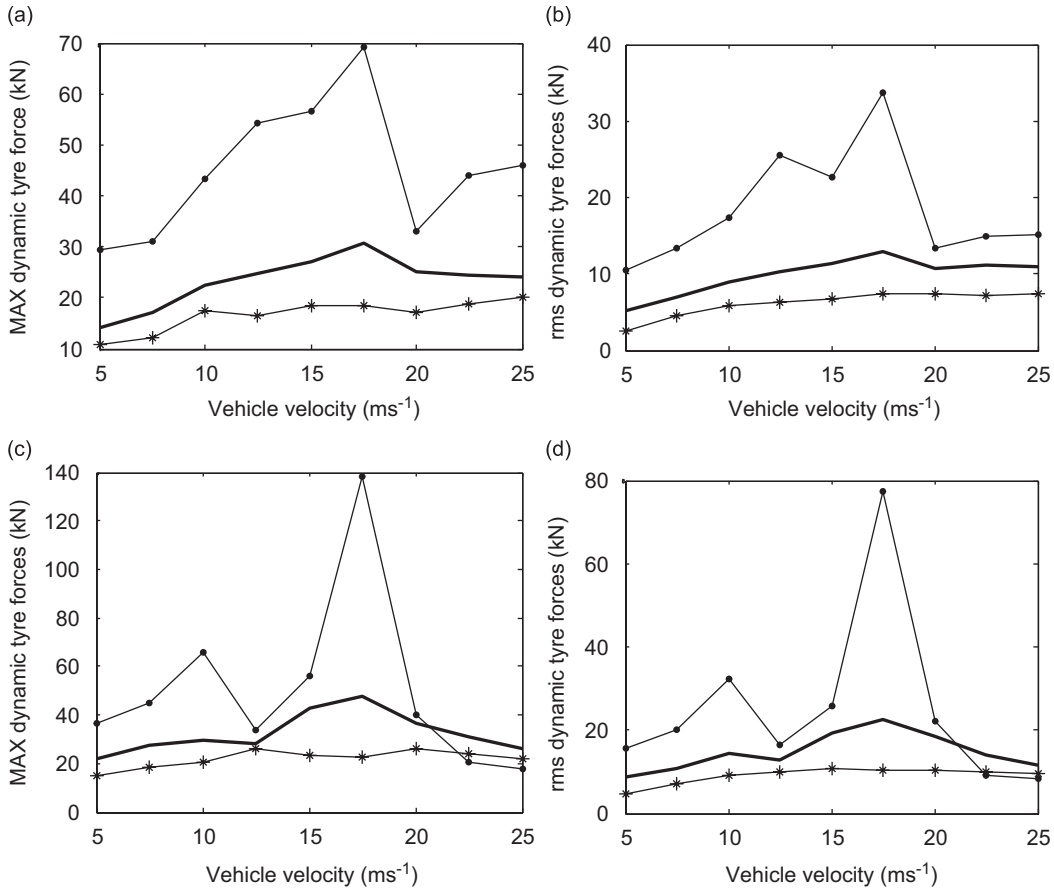

Fig. 10. Dynamic tyre forces: (a) tractor drive axle, (b) tractor drive axle, (c) trailer axle, (d) trailer axle: (——) conventional passive viscous damper, (—●—) passive MR damper (current = 0 A), and (—✳—) semi-active MR damper.

However, the controlled tractor body heave and the pitch acceleration is not any better than that with the passive suspension. In fact, the semi-active suspension increases the peak values of the heave and pitch acceleration. This is not unexpected because the control logic also increases the tractor body pitch acceleration (with a random road input), as depicted in Fig. 6.

3.3. Robustness analysis

Instrumentation noise (due to electromagnetic interference, electrical component damage or any other reason) is a real-life issue. The algorithm robustness to injected white noise into the control loop is therefore examined. An amount of white noise was added to feedback signals, i.e., measured relative velocity and the axle heave acceleration. The noise margin chosen (5%) was based on the fact that internal wiring within a truck is based on sound electrical engineering practice and relevant electromagnetic compatibility standards. Feedback signals are typically hardwired using shielded cables properly grounded (to prevent earth loops), and additional low-pass filtering stages are present in the conditioning on-board electronics.

Furthermore, dedicated circuitries are present and appropriate board layout to increase the immunity to radio-frequency noise. This allows to say that also in a harsh environment, as it is the case of a truck, the noise margin can be reasonably chosen at 5%.

Fig. 14 shows the variation of relative velocity across the tractor drive semi-active damper with and without added noise when the vehicle velocity is $15\,\mathrm{m\,s^{-1}}$.

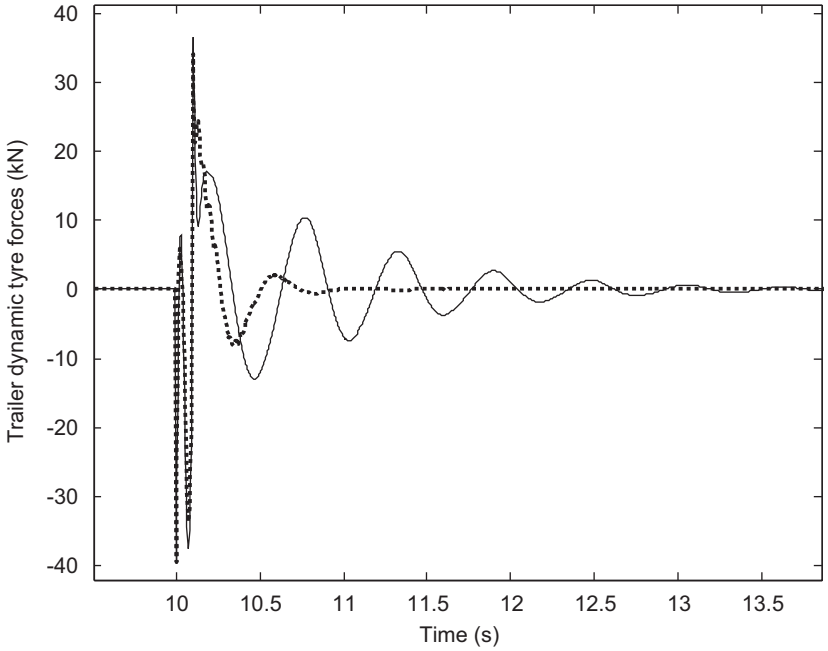

Fig. 11. Trailer dynamic tyre forces due to pothole: (- - - - -) semi-active suspension, and (——) passive suspension.

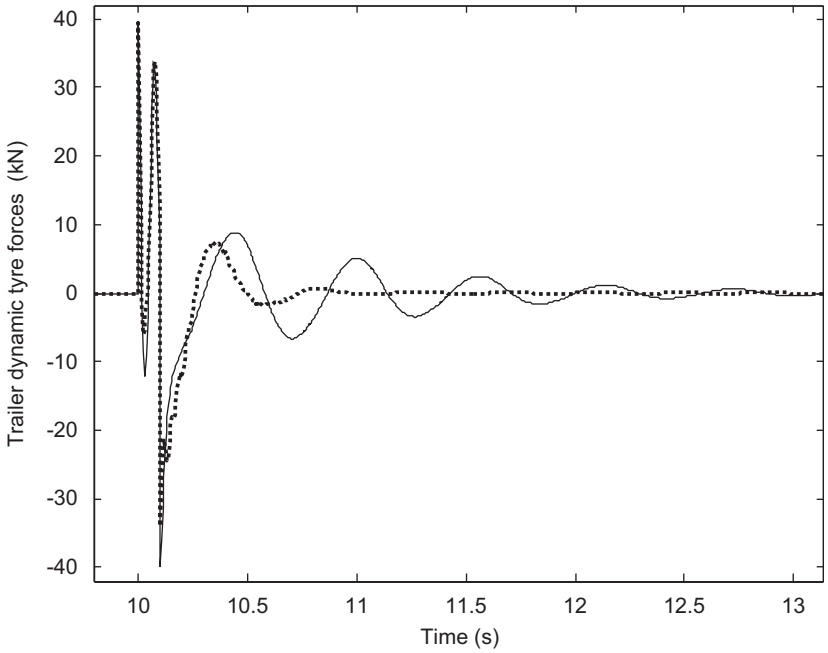

Fig. 12. Trailer drive dynamic tyre forces due to bump: (- - - -) semi-active suspension, and (——) passive suspension.

The system response in respect of trailer chassis acceleration depicted in Fig. 15 is virtually unaffected by the presence of noise; however, the heave and pitch acceleration of the trailer in the semi-active case with noise are moderately increased compared with semi-active control without noise.

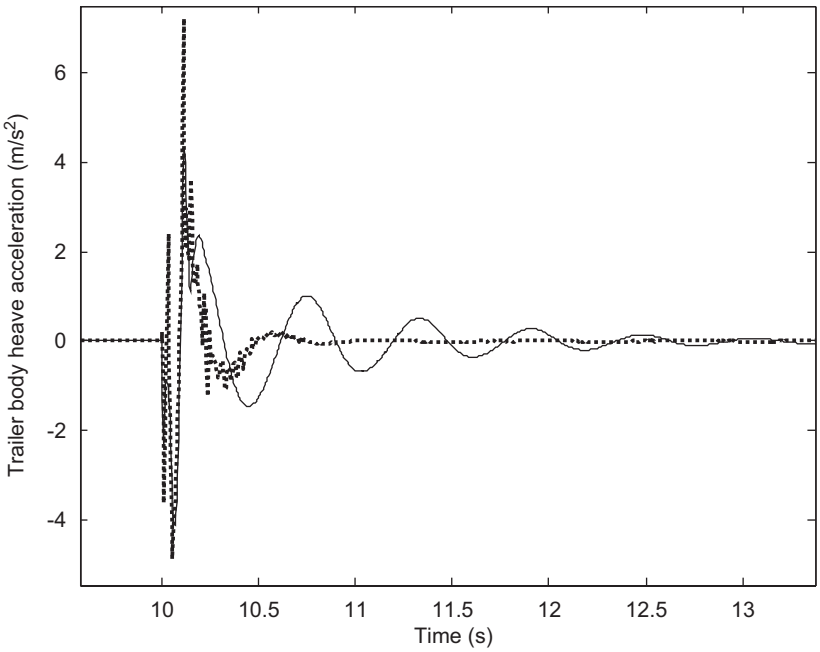

Fig. 13. Trailer body heave acceleration due to pothole: (----) semi-active suspension, (——) passive suspension.

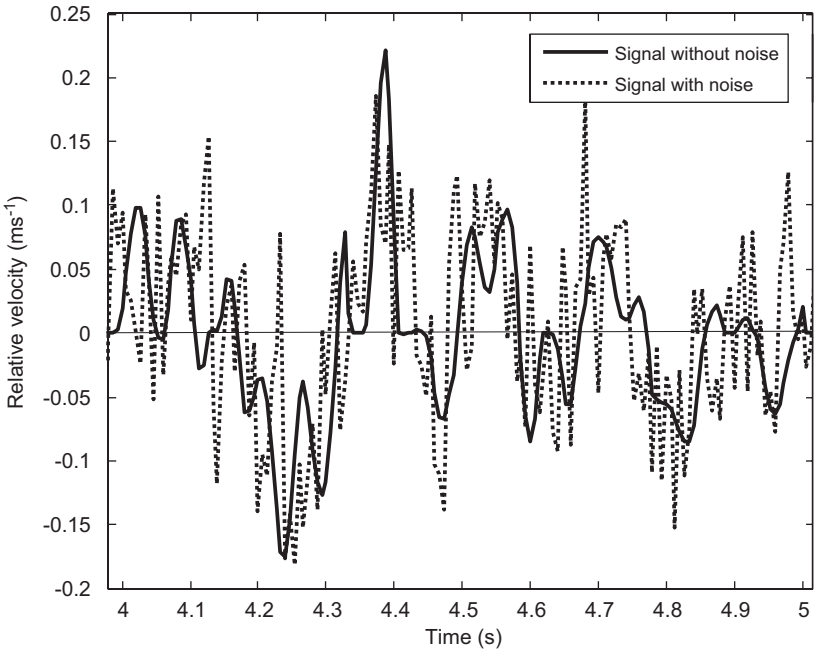

Fig. 14. Relative velocity across the tractor drive semi-active damper: (——) signal without added noise, and (– – –) signal with added noise.

A noisy signal for the semi-active tractor damper contributes to vehicle discomfort by increasing the heave acceleration of the tractor chassis only moderately as compared with the vehicle response without added noise. Consequently, the vehicle response in respect of comfort, using the balance control algorithm, is largely

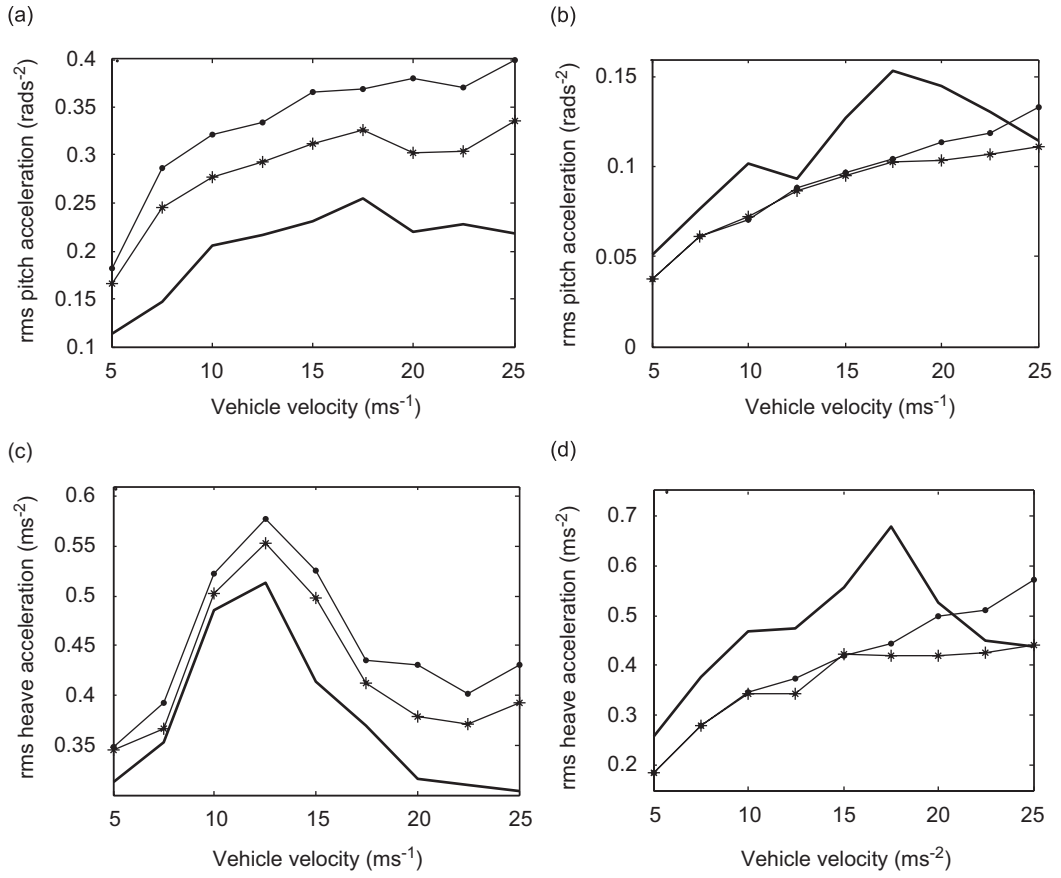

Fig. 15. Chassis acceleration on both vehicle units: (a) tractor chassis, (b) trailer chassis, (c) tractor chassis, (d) trailer chassis: (——) passive, (—●—) semi-active suspension without added noise, and (—✳—) semi-active suspension with added noise.

unaffected by the added noise to the instrumentation signal. A moderate penalty is observed in the heave tractor chassis acceleration between the two semi-active cases.

Next, the rms and MAX dynamic tyre forces on each axle are examined for robustness. Fig. 16 shows that the imposed noise slightly affects the maximum values of the dynamic tyre forces but the rms values are not affected. The maximum dynamic tyre forces of the drive tractor axle are slightly increased by the added noise at 15 and 17.5 $m\,s^{-1}$, while the same values are reduced for high vehicle speeds. Similar performance is observed for the trailer axle, while semi-active control substantially reduces the dynamic tyre forces relative to passive. Consequently, the system performance in terms of dynamic tyre forces, comparing both semi-active cases, is only slightly influenced by the imposed noise to the feedback signals.

A reduction in the number of switches is essential to avoid overheating, wear and reduced component life. A measure of how noise can degrade the overall performance is repeated switching of the controller (chatter). The switches between the ON and OFF states in the two cases are measured as shown in Fig. 17.

For presentation purposes only, the ON-state of the semi-active damper is designated unity while the OFF-state is designated zero. Simulation results show that the semi-active case with the added noise increases chatter as shown in Fig. 17 (time from 3.7 to 4.2 s). Consequently, the added noise limits the life time of the MR damper because the operational temperature of the device increases due to chattering.

3.3.1. Trailer mass variations

Heavy articulated vehicles travel over the pavements both fully loaded and unladen. The effects of the trailer mass variations are vital in terms of road damage. Assuming that the mass of the unladen trailer is

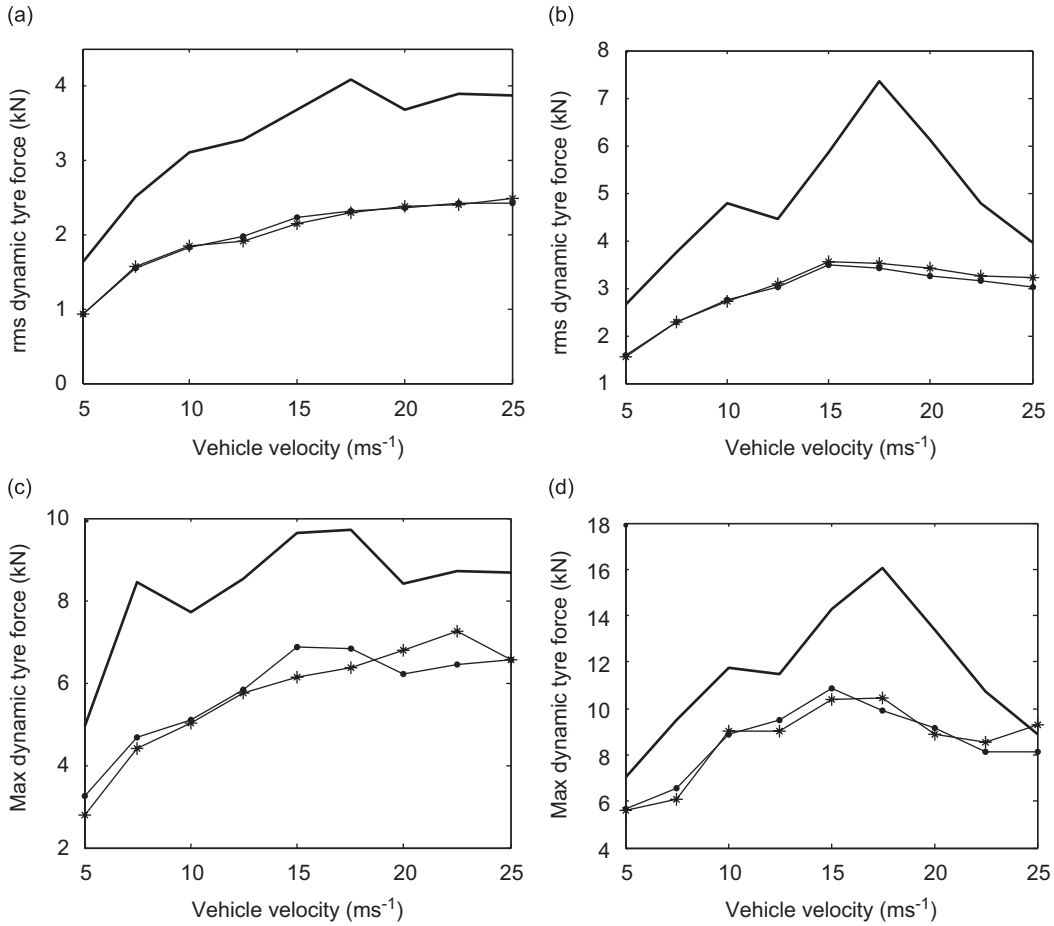

Fig. 16. Dynamic tyre forces of tractor drive and trailer axle: (a) tractor drive axle, (b) trailer axle, (c) tractor drive axle, (d) trailer axle: (——) passive, (—✱—) semi-active suspension without added noise, and (—✱—) semi-active suspension with added noise.

5000 kg, the fully loaded trailer is estimated equal to 12,500 kg for the passive half-vehicle model. A partly loaded trailer with a mass of 8500 kg (for the half vehicle) is also considered.

A range of trailer mass is considered in the simulation process to examine the response of the system between the three cases. Fig. 18 shows the dynamic forces over the speed range 5–25 m s^{-1} for (half) trailer masses of 5000, 8500 and 12,500 kg.

3.3.2. *Tyre stiffness variation of driver tractor wheel*

The tyre is modelled as a spring with high stiffness in order to simulate the vertical tyre motion due to road irregularities. In real operation conditions the tyre pressure is not constant resulting in variation of the tyre stiffness. The tyre stiffness of 2 MN m^{-1} is normally used in the work reported here. Variation of the tyre stiffness of the drive tractor wheel from 1.6 to 2.4 MN m^{-1} shows that the dynamic tyre forces are only slightly affected at low and moderate vehicle velocity (Fig. 19). The system response alters at high vehicle velocities, however, producing larger tyre forces, resulting in higher road damage as expressed by Eq. (13).

3.3.4. *The effect of the semi-active damper response time*

The response time of MR dampers for vehicle applications is an important factor because it determines the effectiveness of the MR damper used. The aim of this work is to assess the effect of the damper response to the vehicle performance.

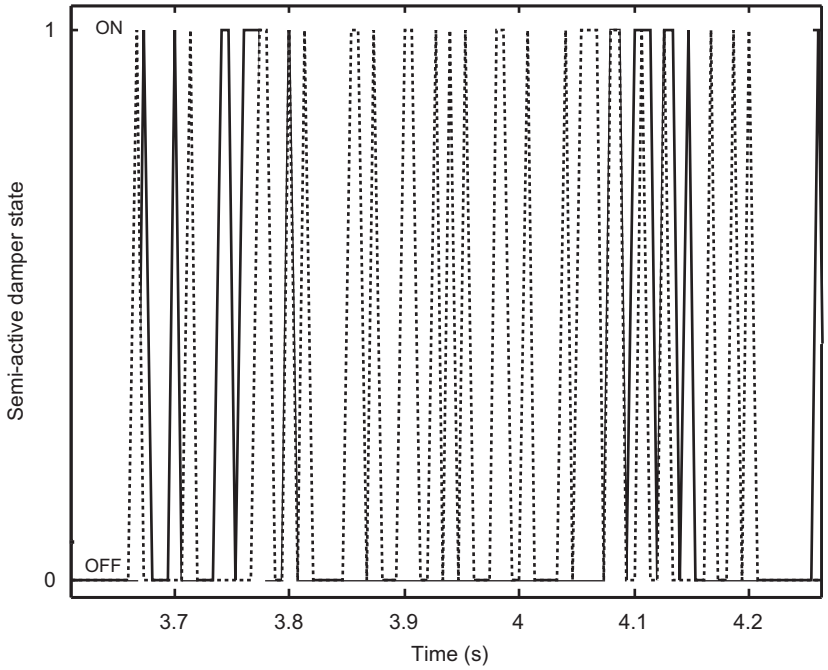

Fig. 17. ON-OFF states of the semi-active damper: (——) semi-active suspension without noise, and (----) semi-active suspension with noise.

The response time can be defined as the time required for the MR damper to reach 64% [36] or 95% [37] of a demanded step change, starting from the initial state. The time response is not affected by the fluid transformation from a mineral oil-like consistency to jelly-like consistency because this time for that event is less than 1 ms [38]. However, extensive experimental work by Koo et al. [37] shows that the time response of the MR damper is affected by several factors such as the response of driving electronics, the applied current, the piston velocity and the system compliance. The MR dampers manufacturing company Lord Corporation [39] also reported that in most MR fluid devices the overall response time is limited by the inductance of the electromagnet and the output impedance of the driving electronics rather than the fluid response.

In the simulation work a first-order lag is employed in the semi-active control schemes in order to emulate the delays which occur in MR dampers. The time constant T_c for a small damper (used for seat control) is quoted as being 25 ms to 95% of its final value [39]. The damper reaches 64% of its final state in one-third of this time, namely 8.3 ms.

A damper designed to produce 160 kN force is quoted [39] as having a time constant of 20 ms to 64% (60 ms to 95%). To allow for the fact that a damper for a freight vehicle would have a time constant greater than one designed for a vehicle seat, but appreciably less than one designed to generate 160 kN, a value of 11 ms to 64% final force was selected and used in this work.

A time constant of 15 ms (to 64%) appears to be an upper bound for a damper suitable for freight vehicle applications.

Simulation results with several different time constants (Fig. 20) indicate that a low time constant (5 ms) is desirable to achieve lower maximum dynamic tyre forces protecting the pavement from fatigue damage, although this may not be practical at present. The results for a time constant of 15 ms (to 64% final value) are naturally poorer than those for 10 ms but not significantly so.

A damper with time constant equal to 20 ms produces larger maximum tyre forces because it cannot change force fast enough to exert the required control force in order to cancel the dynamic tyre forces as specified by Eq. (16). However, this damper generates up to 160 kN force and is used for controlling structural vibrations.

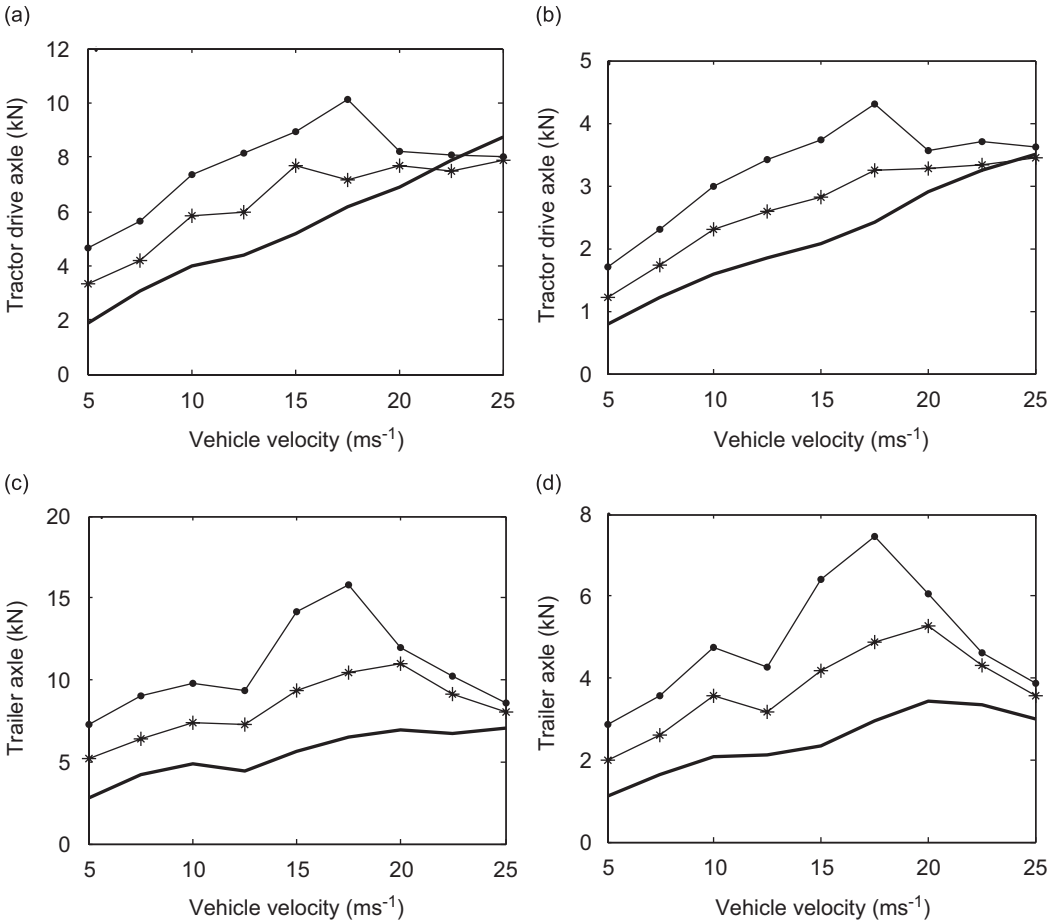

Fig. 18. Dynamic tyre forces due to trailer mass variations: (a) MAX values, tractor, (b) rms values, tractor, (c) MAX values, trailer, (d) rms values, trailer (——) $M_T = 5000$ kg, (—✳—) $M_T = 8500$ kg, and (—●—) $M_T = 12500$ kg.

4. Conclusions

Simulation results indicate that the semi-active vehicle response is overall superior to a conventional passive suspension on both road profiles (smooth and gravel). The MAX and rms values of the dynamic tyre forces are substantially reduced by the control logic and the road damage follows the same pattern as the dynamic tyre forces. A reduction of the trailer chassis acceleration is obtained because the trailer unit is well isolated from the ground irregularities.

Conversely, the tractor chassis acceleration slightly increases because the steer axle is assumed to be equipped with conventional viscous dampers.

Additionally, the simulation results show that the MR damper has poor performance when the applied current is zero (passive operation) due to very low damping provided by the semi-active device. However, this is a situation occurring only in the event of failure of the MR damper.

Partial cancellation of the dynamic tyre forces is also examined to establish the optimum proportion of cancellation on smooth and gravel road profiles while the other control parameters (b_2 and b_3) are kept constant. The results indicate that 75% cancellation of the dynamic tractor drive tyre forces and 50% for the trailer dynamic tyre forces is always preferable in terms of lower road damage. Also, the required damper force with the latter configuration would be significantly lower than in case of 100% cancellation, increasing the power efficiency of the MR damper and the comfort penalty.

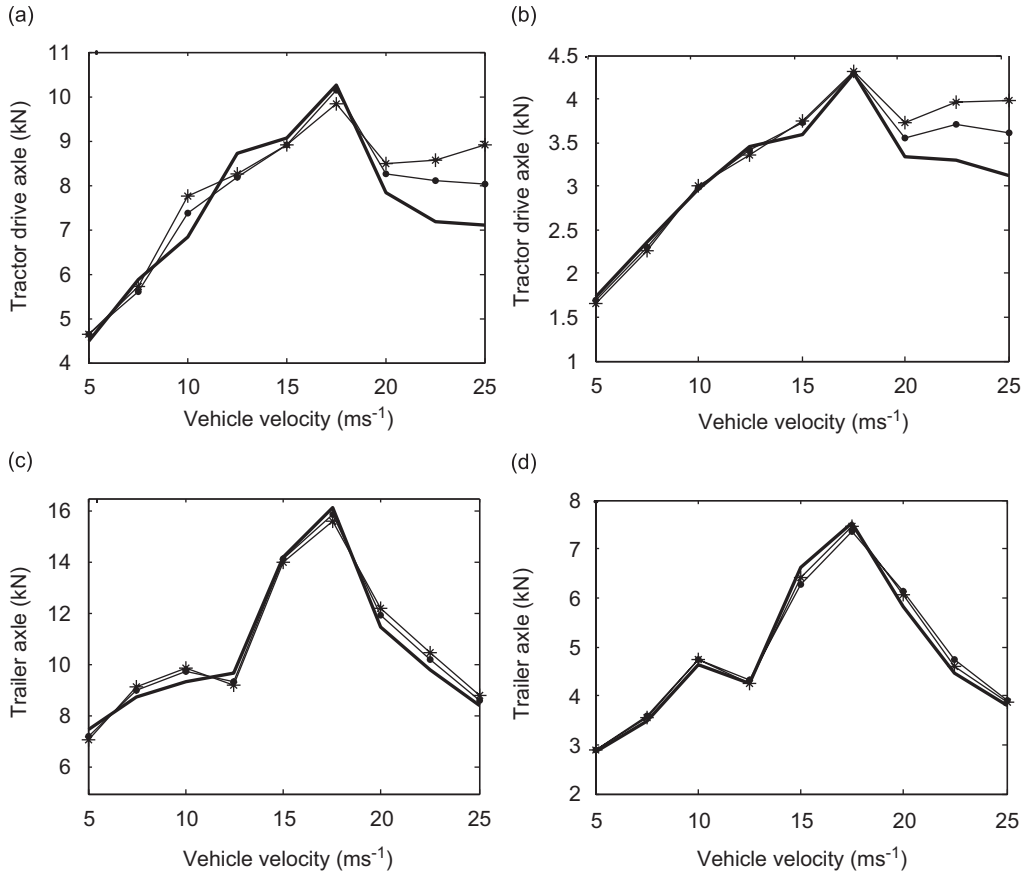

Fig. 19. Dynamic tyre forces due to drive tractor tyre stiffness variations: (a) MAX values, tractor; (b) rms values, tractor, (c) MAX values, trailer, (d) rms values, trailer : (——) $K_{TR} = 1.6\,\mathrm{MN\,m^{-1}}$, (—●—) $K_{TR} = 2\,\mathrm{MN\,m^{-1}}$, and (—✶—) $K_{TR} = 2.4\,\mathrm{MN\,m^{-1}}$.

The vehicle was also tested with pothole and bump input. The results show that the semi-active suspension with the hybrid control algorithm reduces the amplitude of the free oscillations while the peak values of dynamic tyre forces are slightly reduced. Also, the vehicle response is mainly affected by the parameter b_2 rather than the proportion of cancellation.

Chassis accelerations and the rms dynamic tyre forces are slightly affected by imposed noise while the MAX values of the dynamic tyre forces are moderately affected at moderate vehicle velocities. Robustness to sprung mass and unsprung mass variation is also established.

A fast response semi-active damper (time constant equal to 5 ms) is extremely beneficial in reducing dynamic tyre forces. However, this value of time constant is extremely optimistic not only for heavy vehicles but also for passenger vehicles. A realistic value for the current vehicle applications is estimated to vary from 10 to 15 ms.

5. Future work

Future work will address the extension of the control algorithm to a full truck model, investigating also roll performance. Reduction in roll response promises improved handling and protection from roll over of heavy vehicles on roundabouts. The use of fuzzy logic in a passenger vehicle has been shown to reduce switches and hence increase damper life [41]. This could be fruitfully employed in future studies.

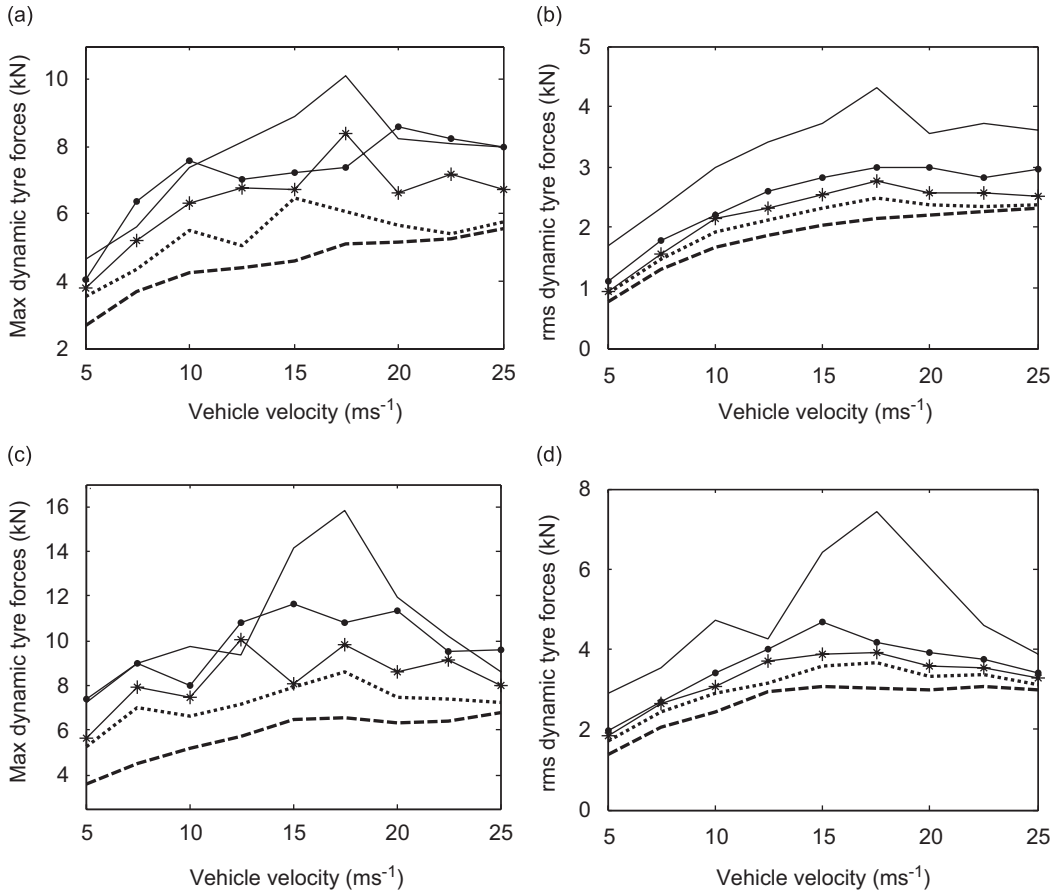

Fig. 20. MAX dynamic tyre forces due to damper response variations: (a) tractor drive axle, (b) tractor drive axle, (c) trailer axle, (d) trailer axle: (——) passive damper, (– – –) $T_c = 5$ ms, (- - - -) $T_c = 10$ ms, (—✳—) $T_c = 15$ ms, (——●——) $T_c = 20$ ms. T_c time to reach 64% of step demand.

Appendix A. Half truck numerical parameters

$C_F = 10\,\mathrm{kN\,s\,m^{-1}}$ (suspension damper rate of steer tractor axle)
$C_R = 27{,}627\,\mathrm{N\,s\,m^{-1}}$ (suspension damper rate of drive tractor axle)
$C_T = 44{,}506\,\mathrm{N\,s\,m^{-1}}$ (suspension damper rate of trailer axle)
$C_5 = 200\,\mathrm{kN\,s\,m^{-1}}$ (damper rate of articulation connection)
$I_T = 18{,}311\,\mathrm{kg\,m^2}$ (tractor pitch inertia)
$I_T = 251{,}900\,\mathrm{kg\,m^2}$ (trailer pitch inertia)
$K_{TF} = 847\,\mathrm{kN\,m^{-1}}$ (tyre spring stiffness of steer tractor wheel)
$K_{TR} = 2\,\mathrm{MN\,m^{-1}}$ (tyre stiffness of drive tractor wheel)
$K_{TT} = 2\,\mathrm{MN\,m^{-1}}$ (tyre suspension stiffness of trailer wheel)
$K_F = 300\,\mathrm{kN\,m^{-1}}$ (spring suspension stiffness of steer tractor axle)
$K_R = 967430\,\mathrm{N\,m^{-1}}$ (spring suspension stiffness of steer tractor axle)
$K_T = 155{,}800\,\mathrm{N\,m^{-1}}$ (spring suspension stiffness of drive tractor axle)
$K_5 = 20\,\mathrm{MN\,m^{-1}}$ (spring stiffness of articulation connection)
$L_1 = 1.2\,\mathrm{m}$ (distance from steer tractor axle to tractor CG)
$L_2 = 4.8\,\mathrm{m}$ (distance from tractor CG to drive tractor axle)
$L_4 = 4.134\,\mathrm{m}$ (distance from tractor CG to articulation point)
$L_5 = 6.973\,\mathrm{m}$ (distance from articulation point to trailer CG)

$L_6 = 4\,\text{m}$ (distance from trailer CG to trailer axle)
$M_C = 4400\,\text{kg}$ (tractor chassis mass)
$M_T = 12{,}500\,\text{kg}$ (trailer chassis mass—fully loaded)
$m_{u1} = 270\,\text{kg}$ (steer tractor unsprung mass)
$m_{u2} = 520\,\text{kg}$ (drive tractor unsprung mass)
$m_{u3} = 340\,\text{kg}$ (trailer unsprung mass)

References

[1] J. Woodrooffe, Heavy truck suspension damper performance for improved road friendliness and ride quality, *Society of Automotive Engineers* (1995) 952636.
[2] D.J. Cole, D. Cebon, Influence of tractor–trailer interaction on assessment of road performance, *Proceedings of the Institution of Mechanical Engineers, Part D, Journal of Automobile Engineering,* (1996).
[3] D.J. Cole, D. Cebon, Truck design to minimise road damage, *Proceedings of the Institution of Mechanical Engineers* 210 (1996) DO6894.
[4] D. Cebon, *Handbook of Vehicle– Road Interaction*, Swets and Zeitlinger, 1996.
[5] D.J. Cole, Fundamental issues in suspension design for heavy vehicles, *Vehicle System Dynamics* 35 (4–5) (1996) 319–360.
[6] F. Queslati, S. Sankar, Optimisation of tractor–semitrailer passive suspension using covariance analysis technique, *Society of Automotive Engineers* (1994) 942304.
[7] S. Vanduri, H. Law, Development of a simulation for assessment of ride quality of tractor–semitrailers, *Society of Automotive Engineers* (1996) 962553.
[8] D.J. Cole, D. Cebon, F.H. Besinger, Optimization of passive and semi-active heavy vehicle suspensions, *Society of Automotive Engineers* (1994) 942309.
[9] I.M. Ibrahim, D.A. Crolla, D.C. Barton, The impact of the dynamic tractor–semitrailer interaction on the ride behaviour of fully-laden and unladen trucks, *Society of Automotive Engineers* (2004) 2004-01-2625.
[10] C.W. Stammers, T. Sireteanu, Vibration control of machines by using semi-active dry friction damping, *Journal of Sound and Vibration* 209 (1997) 671–684.
[11] E. Guglielmino, C.W. Stammers, K.A. Edge, Robust force control in electrohydraulic friction damper systems using a variable structure scheme with non-linear state feedback, *2nd Internationales Fluidtechnisches Kolloquium*, Dresden, Germany, 2000, pp. 163–176.
[12] T. Sireteanu, D. Stancioiu, C.W. Stammers, Use of magnetorheological fluid dampers in semi-active seat vibration control, *Active 2002*, ISVR, Southampton, UK.
[13] E. Guglielmino, C.W. Stammers, D. Stancioiu, T. Sireteanu, R. Ghigliazza, Hybrid variable structure-fuzzy control of a magnetorheological damper for a seat suspension, *International Journal of Vehicle Autonomous Systems* 3 (1) (2005) 34–46.
[14] E. Guglielmino, C.W. Stammers, D. Stancioiu, T. Sireteanu, Conventional and non-conventional smart damping systems for ride control, *International Journal of Vehicle Autonomous Systems* 3 (2/3/4) (2005) 216–229.
[15] S.J. Dyke, B.F. Spencer, M.K. Sain, J.D. Carlson, Modeling and control of magnetorheological dampers for seismic response reduction, *Smart Materials and Structures* 5 (1996) 565–575.
[16] B.F. Spencer, S.J. Dyke, M.K. Sain, D.J. Carlson, Phenomenological model of magnetorheological dampers, *Journal of Engineering Mechanics, American Society of Civil Engineering* 123 (1997) 230–238.
[17] S.B. Choi, S.K. Lee, Y.P. Park, A hysteresis model for the field-dependent damping force of a magnetorheological damper, *Journal of Sound and Vibration* 245 (2001) 375–383.
[18] A. Agrawal, P. Kulkarni, S.L. Vieira, N.G. Naganathan, An overview of magneto- and electro-rheological fluids and their applications in fluid power systems, *International Journal of Fluid Power* 2 (2001) 5–36.
[19] S.P. Kelso, F. Gordaninejad, Magneto-rheological fluid shock absorbers for off-highway, high-payload vehicles, *SPIE Conference on Smart Material and Structures*, San Diego, USA, 1998.
[20] H.S. Lee, S.B. Choi, Control and response characteristics of a magneto-rheological fluid damper for passenger vehicles, *Journal of Intelligent Material Systems and Structures* 11 (1) (2000) 80–90.
[21] Y.K. Lau, W.H. Liao, Design and analysis of magnetorheological dampers for train suspension, *Proceedings of the Institution of Mechanical Engineering, Part F, Journal of Rail and Rapid Transit* 219 (2005).
[22] D. Karnopp, M.J. Crosby, R.A. Harwood, Vibration control using semi-active force generators, *American Society of Mechanical Engineering, Journal of Engineering for Industry* 96 (2) (1974) 619–626.
[23] J. Alanoly, S. Sankar, *A New Concept in Semi-active Vibration Isolation*, Vol. 109, American Society of Mechanical Engineers, New York, 1987.
[24] S. Rakheja, S. Sankar, *Vibration and Shock Isolation Performance of Semi-active 'On– off'' Damper*, Vol. 107, American Society of Mechanical Engineers, New York, 1985.
[25] D.A. Crolla, Vehicle dynamics—theory into practice, *Proceedings of the Institution of Mechanical Engineers, Journal of Automobile Engineering* 209 (1995) 1–12.
[26] Y. Liu, T.P. Waters, M.J. Brennan, A comparison of semi-active damping control strategies for vibration isolation of harmonic disturbances, *Journal of Sound and Vibration* 208 (2005) 21–39.

[27] M. Valasek, W. Kortum, Z. Sika, L. Magdolen, O. Vaculin, Development of semi-active road friendly truck suspensions, *Control Engineering Practice* 6 (1998) 735–744.
[28] J.K. Hendrick, K. Yi, The effect of alternative heavy truck suspensions on flexible pavement response, *Society of Automotive Engineers* (1996) 960937.
[29] K. Yi, B.S. Song, A new adaptive skyhook control of vehicle semi-active suspensions, *Proceedings of the Institution of Mechanical Engineers Part D* 213 (1999) 1.
[30] D. Margolis, C.M. Nobles, Semi-active heave and roll control for large off-road vehicles, *Society of Automotive Engineers* (1991) 912672.
[31] T.D. Gillespie, Heavy truck ride, *Society of Automotive Engineering*, USA (1985) 85001.
[32] T.E.C. Potter, D. Cebon, D.J. Cole, An investigation of road damage due to measured dynamic tyre forces, *Proceedings of the Institution of Mechanical Engineers* 209 (1995) DO2693.
[33] D.H. Wang, W.H. Liao, Modelling and control of magnetorheological fluid dampers using neural networks, *Smart Materials and Structures* 14 (2005) 111–126.
[34] Y.J. Wong, *Theory of Ground Vehicles*, Wiley, New York, 1978.
[35] A.V. Pesterev, L.A. Bergman, C.A. Tan, Pothole-induced contact forces in a simple vehicle model, *Journal of Sound and Vibration* 256 (3) (2002) 565–572.
[36] F.D. Goncalves, Joeong-Hoi Koo, M. Ahmadian, Experimental approach for finding the response time of MR dampers for vehicle applications, *Proceedings of the DETC'03*, American Society of Mechanical Engineering, Chicago, USA, 2003.
[37] Jeong-Hoi Koo, F.D. Goncalves, M. Ahmadian, A comprehensive analysis of the response time of MR dampers, *Smart Material and Structures* 15 (2006) 351–358.
[38] R. Gehm, Delphi improves Cadillac's ride, *Automotive Engineering* 109 (2001) 32–33.
[39] Lord Corporation, MR damper, RD-1005-3, 2003, *Product Bulletin*.
[40] G.I. Tsampardoukas, C.W. Stammers, Semi-active control of a heavy vehicle suspension to reduce road damage, *Proceedings of the XII International Symposium on Dynamic Problems of Mechanics, DINAME 2007*, IIhabela, SP, Brazil.
[41] C.W. Stammers, T. Sireteanu, Fuzzy logic for improved reliability of smart vehicle suspensions, *Fifth International Conference on Quality, Reliability and Maintenance*, Oxford, UK, 2004, pp. 109–112.